Lawrence Berkeley National Laboratory

Title

Numerical Modeling of Gas Migration at a Proposed Repository for Low and Intermediate Level Nuclear Wastes at Oberbauenstock, Switzerland

Permalink

https://escholarship.org/uc/item/2g25k1mm

Author

Pruess, K

Publication Date

1990-03-01

Lawrence Berkeley Laboratory
UNIVERSITY OF CALIFORNIA

EARTH SCIENCES DIVISION

Numerical Modeling of Gas Migration
at a Proposed Repository for Low
and Intermediate Level Nuclear Wastes
at Oberbauenstock, Switzerland

K. Pruess

March 1990

DISCLAIMER

Numerical Modeling of Gas Migration at a Proposed Repository for Low and Intermediate Level Nuclear Wastes at Oberbauenstock, Switzerland

Karsten Pruess

Earth Sciences Division
Lawrence Berkeley Laboratory
University of California
Berkeley, California 94720

March 1990

Abstract

Hydrologic impacts of corrosive gas release from a hypothetical L/ILW nuclear waste repository at Oberbauenstock are explored by means of numerical simulation. A schematic two-dimensional vertical section through the mountain is modeled with the simulator TOUGH, which describes two-phase flow of water and gas in porous and fractured media. Two reference cases are considered which represent the formations as a porous and as a fractured-porous (dual permeability) medium, respectively. Both cases predict similar and rather modest pressure increases, from ambient 10 bars to near 25 bars at the repository level. These results are to be considered preliminary because important parameters affecting two-phase flow, such as relative permeabilities of a fractured medium, are not well known at present.

Table of Contents

List of Figures

List of Tables

Nomenclature

C	heat capacity, J/kg°C
D	diffusivity, m^2/s
F	flux, kg/s · m^2 for mass, W/m^2 for heat
h	specific enthalpy, J/kg
k	permeability, m^2
k_r	relative permeability, dimensionless
K	thermal conductivity, W/m°C
M	accumulation terms, kg/m^3 for mass, J/m^3 for heat
n	unit normal vector
P	pressure, Pa
q	sink/source rate, kg/m^3·s for mass, W/m^3 for heat
S	saturation (volume fraction), dimensionless
t	time, s
T	temperature, °C
u	specific internal energy, J/kg
V	volume, m^3
x	distance coordinate, m
X	mass fraction, dimensionless
z	elevation coordinate, m

Greek

β	phase (β = liquid, gas)
Γ	area, m^2
$\delta_{\beta g}$	1 for β = g, 0 otherwise
ϕ	porosity, dimensionless
ρ	density, kg/m^3
κ	component (κ = 1: water; κ = 2: air or hydrogen; κ = 3: heat).
μ	viscosity, Pa·s
τ	tortuosity factor, dimensionless
θ	exponent in temperature-dependent diffusivity, dimensionless

Subscripts

a	air
cap	capillary

g   gas

l liquid

n   volume element (grid block) index

R   rock

1.0. INTRODUCTION

For a number of years the "Nationale Genossenschaft fuer die Lagerung radioaktiver Abfaelle" (NAGRA) has been developing a repository project for geologic disposal of low- and intermediate-level radioactive wastes. Recent site investigations have focussed on a site in the Oberbauenstock mountain (NGB 85-07; NGB 85-08; Resele and Tripet, 1985).

A nuclear waste repository will contain large amounts of concrete, metals, and organic materials in contact with groundwater (NGB 85-07). Detailed studies have indicated that corrosion of the metals and microbial degradation of the organic materials will evolve large amounts of gas (NGB 85-07; Neretnieks, 1985; Rasmuson and Elert, 1986; Wiborgh, Hoeglund, Pers, 1986), the chief constituents being hydrogen, methane, and carbon dioxide. Additional relatively minor amounts of gases will be generated from radiolysis of water.

The expected gas release raises several concerns. From the data given by Wiborgh et al. (1986) it can be estimated that gas pressures in the repository could build up to levels of several hundred bars unless specific design provisions are made for gas venting. Such pressures could breach the system of engineered barriers and compromise the integrity of the repository. On the other hand, gas escaping from the repository volume could alter existing groundwater flow paths in the host rock, and thereby impact on the travel time of potential contaminants to the biosphere.

The present study is a first preliminary attempt to evaluate, by means of computer simulation, the gas release from the repository and its effects on pore pressures and groundwater flow in the host rock. We give a brief summary of previous work on the hydrogeology of the Oberbauenstock site, and on the issues relating to gas release. We then proceed to define two reference cases for computer simulation of two-phase (gas-liquid) fluid flow in the host rock, which model the formations as a porous and as a fractured-porous medium, respectively. Both cases are highly schematic in nature and are not intended to provide realistic results for a potential

repository at Oberbauenstock. The chief objectives of the simulations are to test the performance of our numerical simulator, and to establish a baseline for communication with NAGRA scientists, so that important issues can be identified and more realistic models be developed.

2.0. DEFINITION OF REFERENCE CASES

The Swiss research program for a geologic repository for low and intermediate level nuclear wastes has developed a large number of specialized investigations which have been summarized in two recent reports (NGB 85-07; NGB 85-08). The present study builds on the results of these investigations. We utilize conceptual models and parameters developed by NAGRA to define a detailed numerical model for two-phase flow of groundwater and hydrogen gas in the vicinity of a potential nuclear waste repository at Oberbauenstock. The numerical model is implemented through a modified version of the simulation program "TOUGH" (Pruess, 1987), which describes non-isothermal flow of water and air in porous or fractured media. For reference a summary description of the TOUGH simulator is given in the appendix. In the modified version used in the present work the air component of TOUGH was replaced by hydrogen.

The parameters of the porous medium reference case are given in Table 1, while additional data for the fractured-porous medium case are given in Table 2. We will here give a brief summary of data sources and considerations pertaining to these parameters.

2.1. Model Domain

We model the same two-dimensional vertical section through Oberbauenstock for which single phase groundwater flow calculations had previously been made by NAGRA (NGB 85-08). The choice of the 2-D section was substantiated by NAGRA's three-dimensional modeling work, which indicated that the hydraulic potential was slowly varying in the direction parallel to the shore of Lake Uri. Figure 1 (from NGB 85-07) shows the stratigraphy of the section. The potential repository horizon is located in a thick (300 - 400 m) layer of Valanginian marl of low permeability. This formation is sandwiched between more permeable limestone formations above and below. The model domain as shown in Figure 2 (from NGB 85-08) is bounded from above

Table 1. Parameters for the porous medium reference case

Model domain[*]

upper boundary:	coordinates of highest point $(x, z) = (0\ m, 300\ m)$
	slope of western flank $\alpha_1 = 86°$
	slope of eastern flank $\alpha_2 = 67°$
western boundary:	$x = -2125\ m$
lower boundary:	$z = -300\ m$

Boundary conditions

bottom:	no flow	
western:	no flow	
upper:	western flank	$P = 9810 \times (220 - z) + 1 \times 10^5$ $(z < 220\ m)$[†]
		$P = 1 \times 10^5$ $(z > 220\ m)$
	eastern flank	$P = 1 \times 10^5$ $(z > 0\ m)$
		$P = -9810 \times z + 1 \times 10^5$ $(z < 0\ m)$

Initial conditions

temperature:	10°C
pressure:	corresponding to steady-state
	flow for the boundary conditions
	given above

Formation parameters

domain	extent	permeability	porosity
Valanginian marl	$z > -150\ m$	10 μd	3 %
limestone	$z < -150\ m$	10 md	3 %
repository	$-1125\ m < x < -425\ m$	1 md	3 %
	$10\ m < z < 70\ m$		
Seelisberg tunnel	$90\ m < x < 340\ m$	1 md	3 %
(assumed collapsed)	$-50\ m < z < 190\ m$		

Relative permeability
(Corey's curves)

liquid phase:	$k_{rl} = [S*]^4$
gas phase:	$k_{rg} = (1 - S*)^2 (1 - [S*]^2)$
where	$S* = (S_l - S_{lr})/(1 - S_{lr} - S_{gr})$
	$S_{lr} = 0.3,\ S_{gr} = 0.05$

Gas release rates[§]

$Q_g = 3.339 \times 10^{-7}\ kg/s$	for $t < 20$ years
$Q_g = 1.484 \times 10^{-7}\ kg/s$	for $t > 20$ years

[*] see Fig. 2 and Table 7-5 of report NGB 85-08.

[†] pressures in Pascals

[§] 1/466 of total repository rate, based on average cavern length of 466·m.

Oberbauenstock

WSW

Ⓐ Profil P-P'

ENE

Ⓐ

Profil Q-Q'

m ü.M.

1600

Modell-Datensatz für Projekt Gewähr 1985.
Geographische Angaben bilden kein Präjudiz
für die erst später zu treffende Wahl eines
Endlagerstandorts.

Profil R-R'

1400

1200

1000

Profil S-S'

800

Tablet Kantonsstrasse
nach Bauen

600

Bergröhre Seeröhre

Kote potentielle
Lagerzone

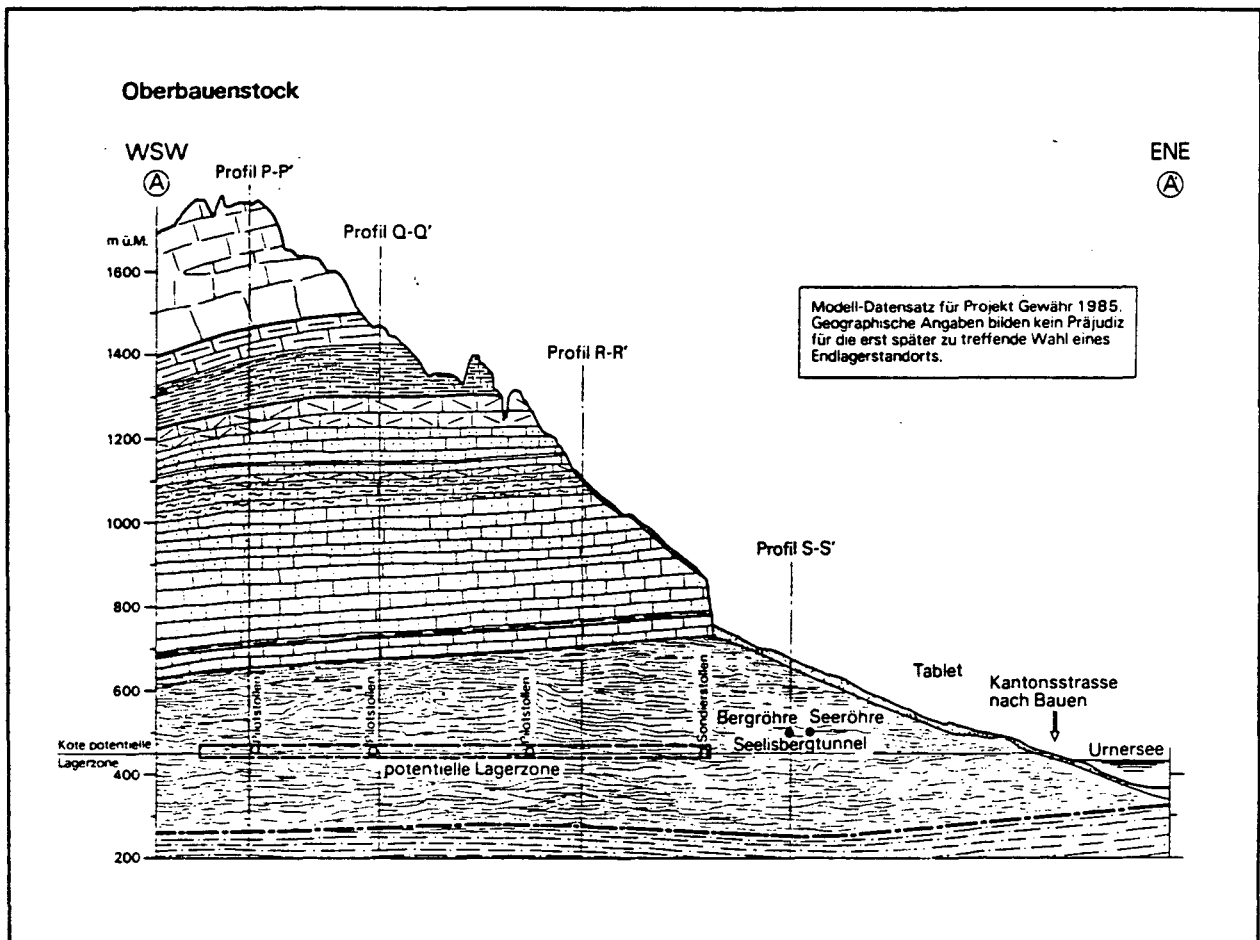400 potentielle Lagerzone

Seelisbergtunnel

Urnersee

200

Figure 1. Vertical cross section through Oberbauenstock (from NGB 85-07).

by the contact to the limestone on the western flank, and by the steeply dipping ground surface in the east. The lower boundary of the model is beneath a layer of limestone which has relatively high permeability (see below). The western boundary is placed somewhat arbitrarily at a distance of 1 km from the proposed western boundary of the repository.

2.2. Computational Grid

For the porous medium reference case, the flow domain is partitioned into essentially rectangular volume elements or "grid blocks." The grid as specified in Table 3 consists of rectangular blocks, with suitable cutoff at the sloping top boundaries. The grid is similar to that used by NAGRA for 2-D model studies (NGB 85-08). A preprocessor program was written for the grid generation; minor adjustments in nodal locations and grid block interfaces were made by hand to properly account for the pinchout in the lower eastern corner. Including all boundary blocks and connections, the grid consists of 328 elements with 544 interfaces between them. A plot of grid block locations is given in Figure 3. For convenience grid thickness has been chosen as 1 m.

For the fractured-porous medium case each of the volume elements of the porous medium grid was further partitioned into two regions, corresponding to fracture and rock matrix domains, respectively. A more detailed discussion of issues of flow geometry and gridding for the fractured-porous medium is given in section 4, below.

2.3. Formation Parameters

NAGRA has undertaken a variety of theoretical, laboratory, and field studies to estimate natural groundwater flow and large-scale permeability and porosity in the potential host formations at Oberbauenstock. Laboratory measurements on a small sample of Valanginian marl yielded an extremely small permeability of 0.026 μd and a porosity of 3.1% (NGB 85-07). Field scale permeability is dominated by networks of fractures and faults. A detailed study of the geometric and hydrologic properties of the fracture networks at Oberbauenstock was presented by Resele and Tripet (1985). These authors estimated large-scale permeability of the host rock as approximately 10 μd. In the vicinity of mined openings (e.g., drifts, tunnels) permeability is

Table 2. Parameters for fractured-porous medium description

Domain	Fracture permeability	Matrix permeability	Fracture porosity	Matrix porosity
Valanginian marl	10 μd	0.1 μd	1%	3%
Chalk	10 md	1 md	1%	3%
Repository	1 md	0.1 md	1%	3%
Seelisberg tunnel (assumed collapsed)	1 md	0.1 md	1%	3%

Table 3. Basic computational grid

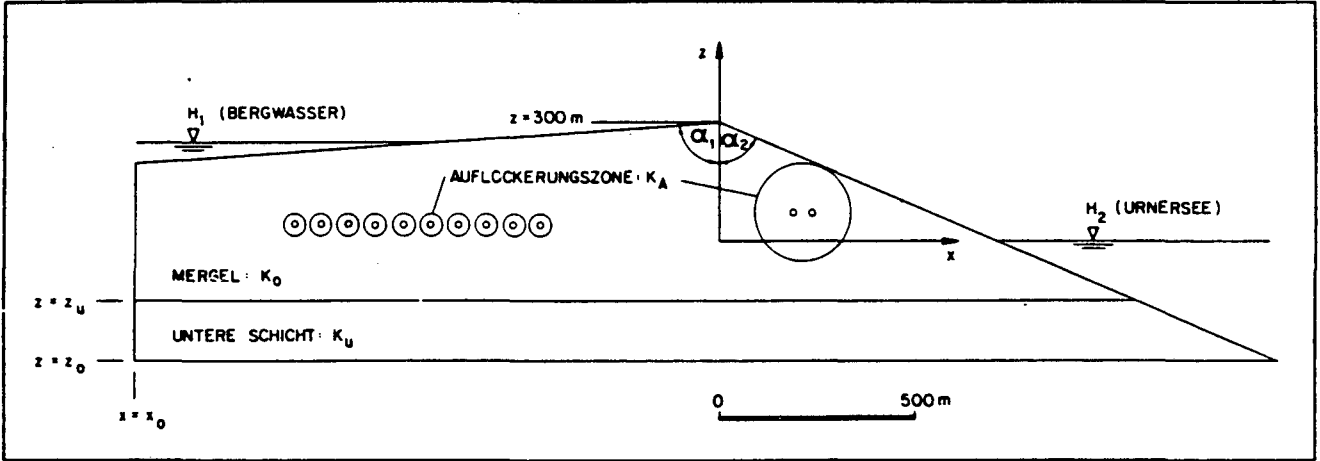| Row #	x-coordinate of left grid boundary (m)	Δx (m)	Column index	z-coordinate of lower grid boundary (m)	Δz (m)
1	- 2125	250	A	- 300	100
2-4	- 1875	3 x 200	B	- 200	50
5	- 1275	100	C	- 150	50
6, 7	- 1175	2 x 50	D	- 100	50
8-15	- 1075	8 x 75	E	- 50	60
16, 17	- 475	2 x 50	F	10	60
18-21	- 375	4 x 100	G	70	60
22	25	65	H	130	60
23-27	90	5 x 50	I	190	60
28	340	73.5	J	250	50
29-38	413.5	10 x 100			

Figure 2. Schematic diagram of a two-dimensional model for groundwater flow developed by NAGRA (from NGB 85-08).
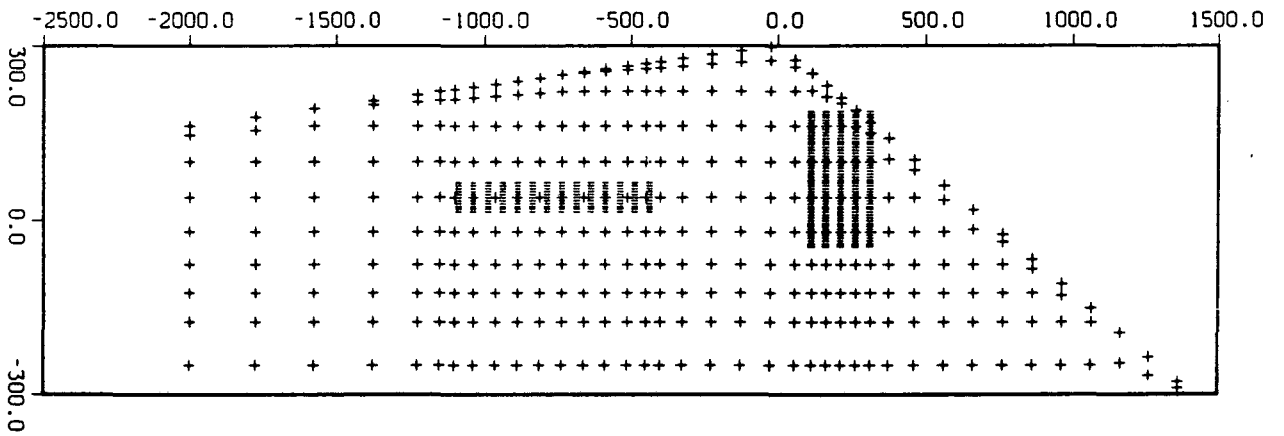

Figure 3. Grid block locations for the model developed in the present study (shaded areas indicate the zones of higher permeability around the repository and Seelisberg tunnel).

expected to be enhanced by perhaps two orders of magnitude because of stress relief. For our porous medium reference case we have adopted permeability and porosity values identical to those used in the base case of NAGRA's 2-D model (NGB 85-08). A highly idealized representation of fracture geometry, loosely based on the analysis of Resele and Tripet (1985), was adopted for the fractured-porous medium case (see section 4).

2.4. Boundary and Initial Conditions

The boundary conditions imposed on the model domain are identical to those used in previous 2-D modeling studies by NAGRA (NGB 85-08). Initial conditions are a temperature of 10°C throughout the flow domain, and steady-state pressures for the given boundary conditions. The steady-state pressure field was generated by means of a TOUGH simulation, in which arbitrary initial pressure conditions were run to steady state for the applied boundary conditions. The initial pressures for the porous and fractured-porous medium cases are very nearly identical, and are indistinguishable on the scale of the contour plot in Figure 4.

2.5. Relative Permeability and Capillary Pressure

The relative permeability and capillary pressure characteristics of fractured rocks are poorly understood, and no data are available for the formations at the Oberbauenstock site. In their estimation of gas transport at Oberbauenstock, Wiborgh et al. (1986) have utilized published capillary pressure data for three different porous media (sandstone, dolomite, limestone). The applicability of these data to fractured Valanginian marl is questionable. Further uncertainties are introduced when relative permeabilities are derived from capillary pressure data, as the relationship between the two involves hypothetical models of pore space geometry. For this first exploratory study we have decided not to use the gas phase relative permeabilities obtained by Wiborgh et al. (they provide no liquid relative permeability data). Instead we have taken standard relative permeability functions and parameters for two-component two-phase systems (Corey, 1954).
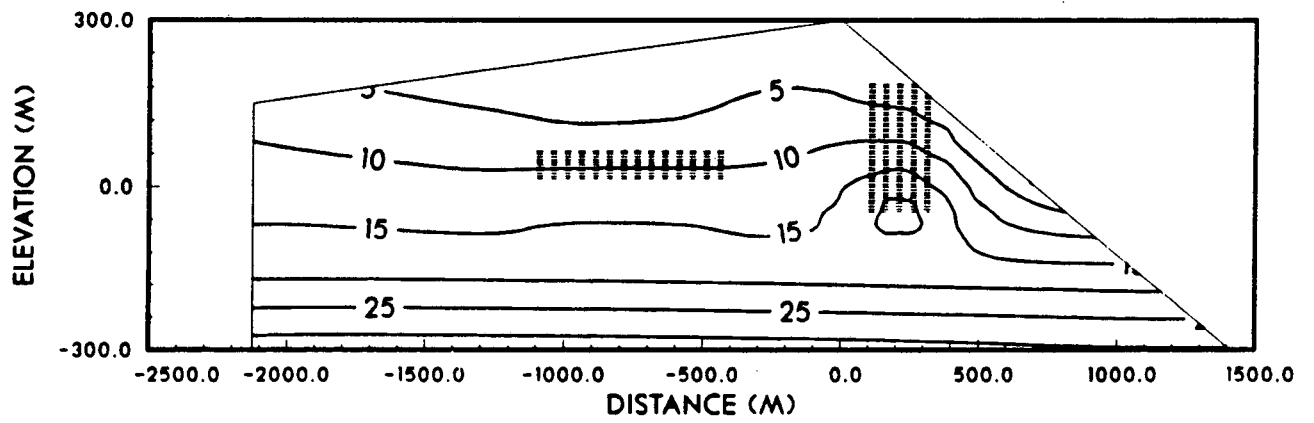
Figure 4. Contour diagram of initial steady state groundwater pressures (in bars).

In rocks with small pores capillary pressures can be strong, reaching tens of bars at low values of liquid saturation (Wiborgh et al., 1986; Pruess et al., 1988). Test calculations revealed that gas pressurization effects would be large, so that capillary pressure effects may not be major. Therefore, given the lack of any specific data on applicable capillary pressure for the formations under study, it was decided to simply ignore capillary pressure for the reference case calculations.

It is anticipated that relative permeabilities and capillary pressures constitute major unknown parameters with a potentially large impact on predicted fluid pressures and flows. These issues will have to be addressed in future studies.

2.6. Gas Release Rates

Total gas release rate for the entire repository has been estimated as 1.8×10^{-3} m^3 (STP)/s for t < 20 years, and as 8.0×10^{-4} m^3(STP)/s thereafter (NTB 85-17, p. 56). From the data given in NGB 85-07, the total length of the storage caverns is approximately 4660 m. With 10 caverns in parallel, average cavern length is 466 m, so that we allocate 1/466 of total gas generation rate to our 1 m thick model section. For specification of a mass release rate the density of hydrogen gas at T = 10°C, P = 1 bar, is needed, which is 0.08645 kg/m^3 (Vargaftik, 1975).

2.7. Fluid Data

Thermophysical properties of water were taken from the steam table equations as given by the International Formulation Committee (1967). Following the approximation made in previous estimations of gas effects (Wiborgh et al., 1986; Rasmuson and Elert, 1986), all gas generated in the repository is assumed to be hydrogen. This is modeled as an ideal gas; the thermophysical properties needed are given in Table 4. (For the present problem TOUGH is run in isothermal mode, and it is not necessary to specify a heat capacity for the gas.)

3.0. RESULTS FOR THE POROUS MEDIUM CASE

Simulated results for the porous medium reference case are shown in Figures 5-12. In

Table 4. Thermophysical properties of hydrogen

density at P = 1 bar	experimental[*]	ideal gas law[†]
T = 280 K	.086546 kg/m^3	.08660 kg/m^3
T = 300 K	.080776 kg/m^3	.08083 kg/m^3

viscosity[*]

	T = 0°C	T = 100°C
P = 1 bar	8.40×10^{-6} Pa·s	10.33×10^{-6} Pa·s
P = 100 bar	8.57×10^{-6} Pa·s	10.44×10^{-6} Pa·s

solubility in water at P = 1 bar[§]

T = 0°C	2.14 cm^3/100 g H$_2$O
T = 25°C	1.91 cm^3/100 g H$_2$O

Solubility at higher pressures is computed from Henry's law, with Henry's constant at T = 10°C obtained by linear interpolation from the above solubility values at 0 and 25°C, respectively.

[*]from Vargaftik (1975).

[†]universal gas constant R = 8314 J/mol/°C; molecular weight of hydrogen 2.0160 (Vargaftik, 1975).

[§]after Rasmuson and Elert (1986).
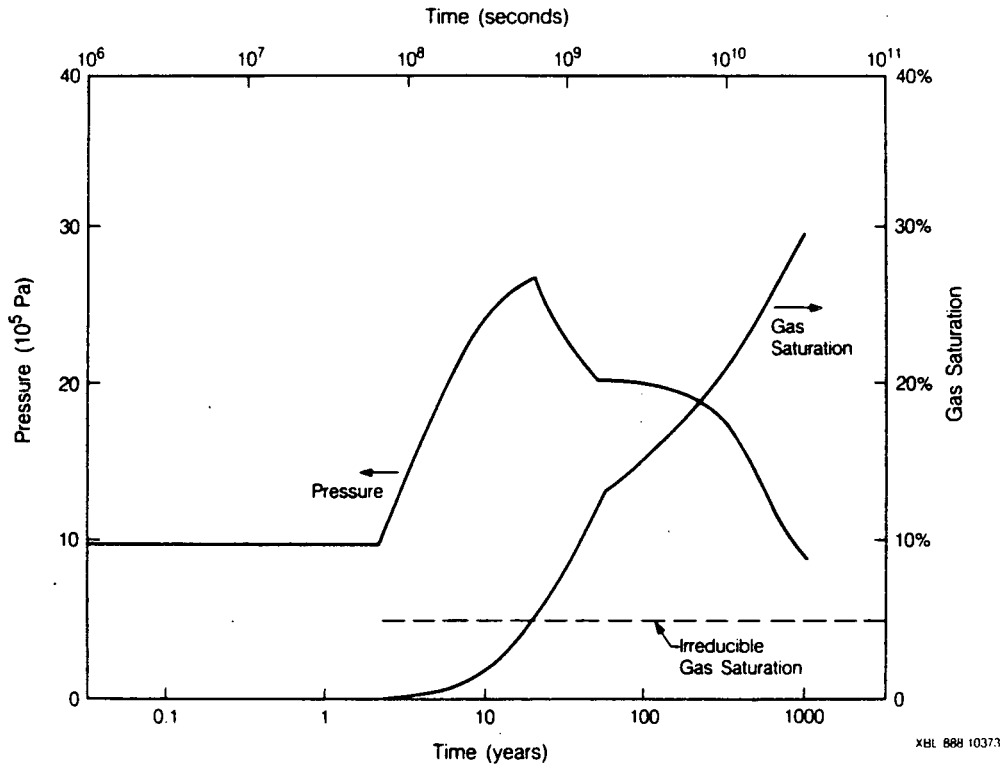
Figure 5. Predicted temporal evolution of gas pressures and saturations at the repository level in porous medium model.
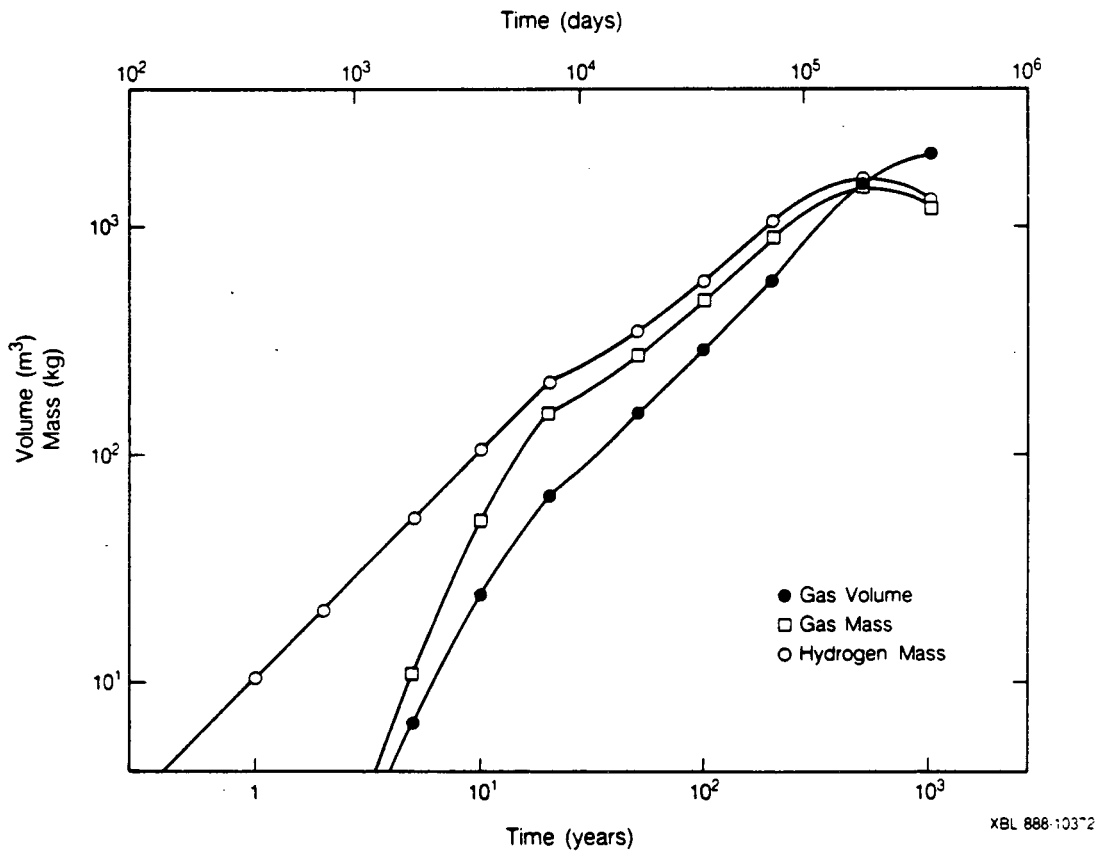
Figure 6. Predicted temporal trends of gas volume and mass in the model domain (porous medium model).

Figure 7. Simulated gas saturations (in percent) at t = 20 years (porous medium model).

Figure 8. Simulated pore pressures (in bars) at t = 20 years (porous medium model).

Figure 9. Simulated gas saturations (in percent) at t = 200 years (porous medium model).

Figure 10. Simulated pore pressures (in bars) at t = 200 years (porous medium model).

Figure 11. Simulated gas saturations (in percent) at t = 1000 years (porous medium model).

Figure 12. Simulated pore pressures (in bars) at t = 1000 years (porous medium model).

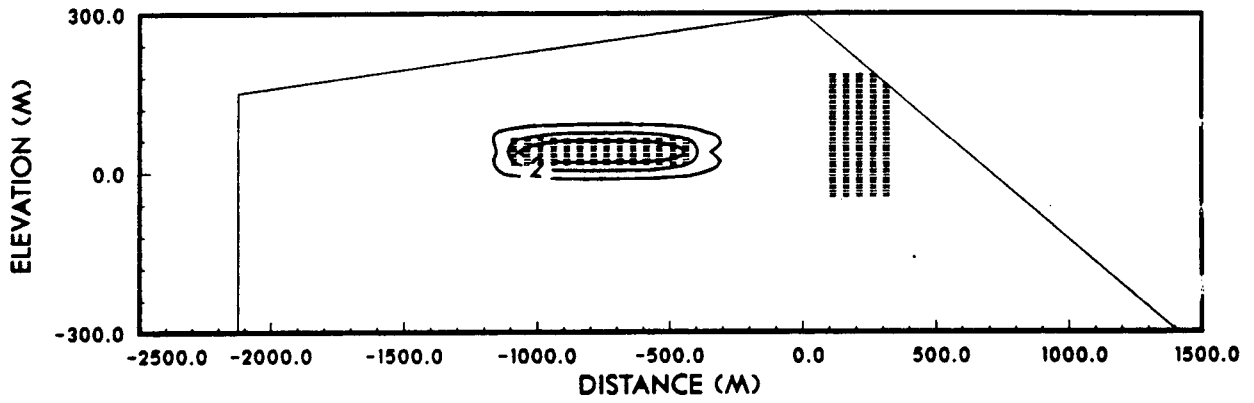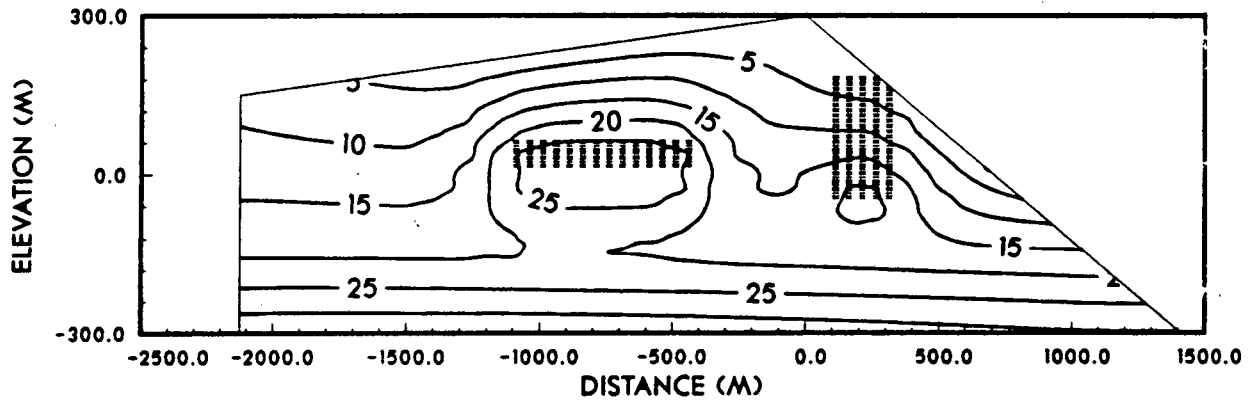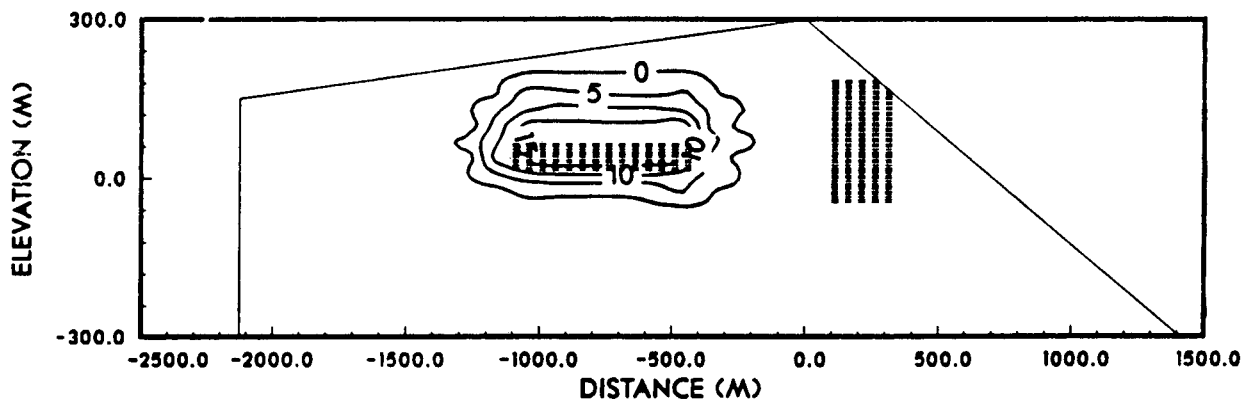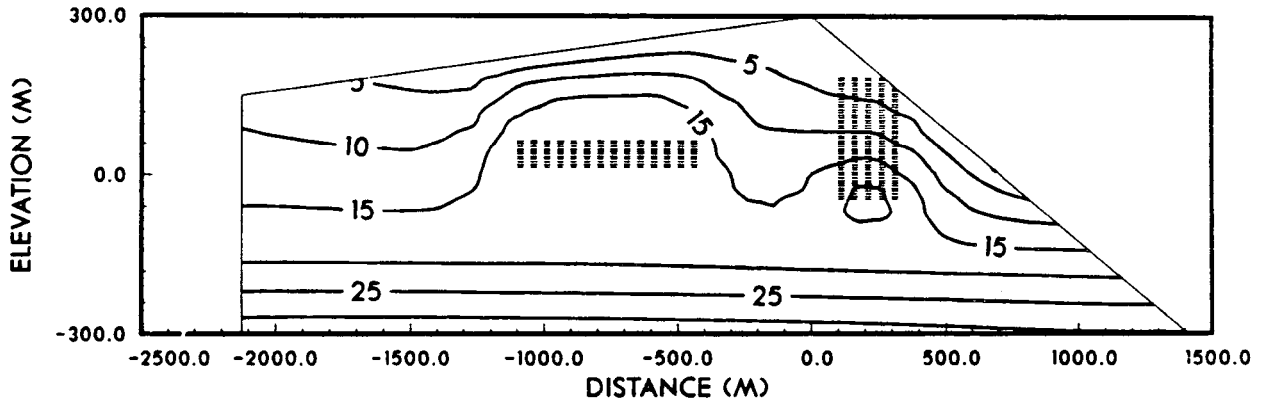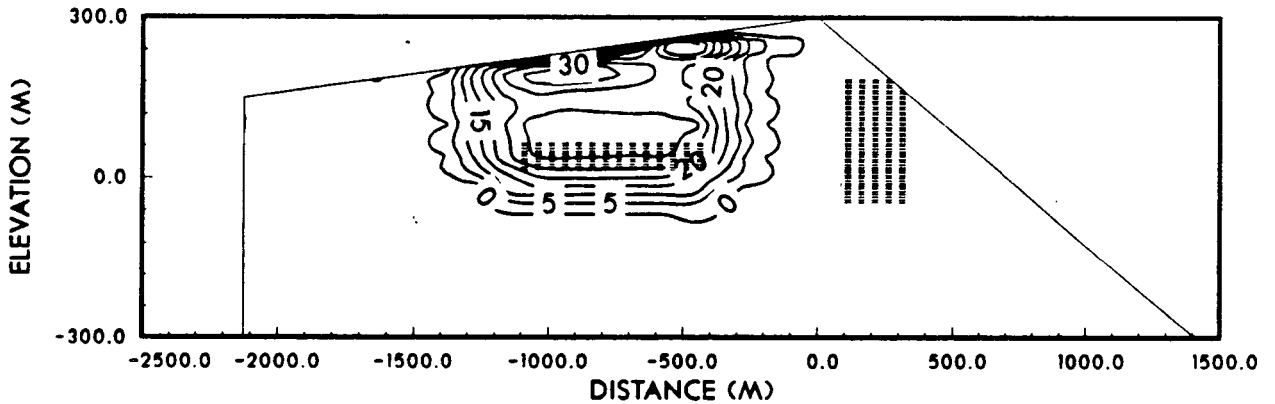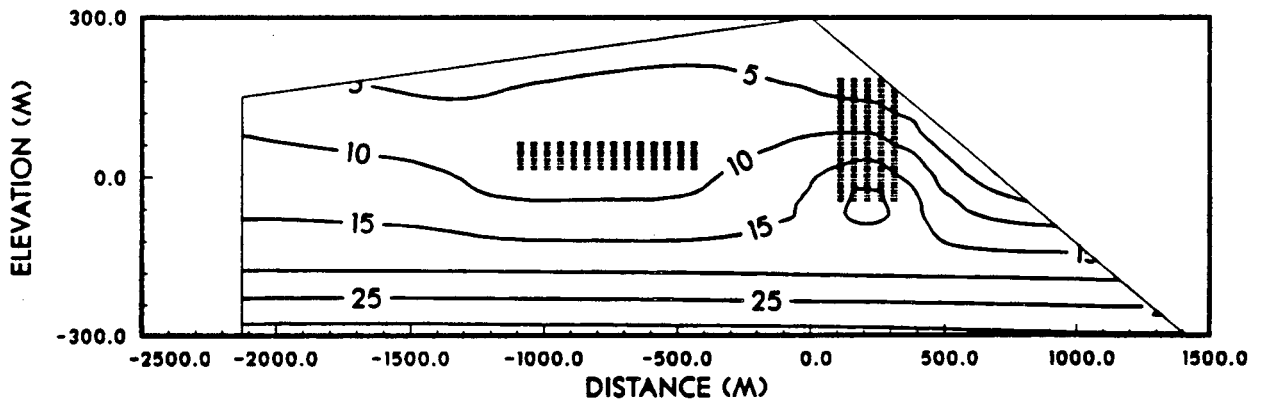agreement with previous analysis (Rasmuson and Elert, 1986) our simulation shows that dissolution and removal of gas by flowing groundwater occurs at a rate which is smaller than the rate of gas generation. In our model it takes approximately 2.5 years for hydrogen to exceed the solubility limit. Subsequently, a free gas phase evolves in the repository grid blocks, which is accompanied by an increase in fluid pressure (see Figure 5). Gas mass at early time is much smaller than hydrogen mass, indicating that initially most of the hydrogen is dissolved in the water (Figure 6). Gas saturation in the repository grid blocks remains below the irreducible value (here assumed 5 %) for almost 20 years. During this period gas remains confined to the repository grid blocks (see Figure 7). Fluid pressures attain a local maximum around the gas sources (see Figure 8), but remain close to the steady-state values otherwise (compare Figure 4).

Gas phase saturation exceeds the irreducible limit and gas becomes mobile just prior to the rate change at t = 20 years. Subsequently, gas flows away from the repository. Together with the sharp drop in gas generation rate, this leads to a strong pressure decline. After approximately 60 years the flow system has adjusted to the new lower gas rate, and enters a period of slow pressure decline with a continued slow increase in gas saturation (Figures 5 and 6). After 200 years the gas bubble around the repository has expanded almost to the boundary of the flow domain (Figure 9), while pressures have declined closer to the steady state pressures prior to gas release (compare Figures 10 and 4). The mass of gas and hydrogen (gaseous as well as dissolved) reaches a maximum at about 500 years (Figure 6). At later time hydrogen is removed from the top boundary of the system at a larger rate than it is being generated in the repository, so that total gas and hydrogen inventories decline. This is accompanied by pressure decline so that gas saturation and total gas volume continue to increase even as gas mass is decreasing (Figures 5 and 6). After 1000 years gas saturation at the repository level has reached almost 30 %, while maximum saturation near the top boundary is approximately 33 % (Figure 11). The pressure at the repository level has declined slightly below the initial steady-state value (Figure 5; see also the downward depression of the P = 10 bar contour in Figure 12).

Hydrogen mass balances for the entire model domain are given in Table 5. It is seen that

Table 5. Total hydrogen mass (kg) in 2-D Oberbauenstock porous medium model

Time (years)	TOUGH-simulation	Total release
1	10.37	10.54
2	20.91	21.08
5	52.64	52.70
10	105.4	105.4
20	211.8	210.8
50	352.1	351.3
100	586.3	585.4
200	1054.6	1053.7
500	1645.7	2458.7
1000	1357.5	4800.0

for t < 200 years, the hydrogen inventory in the system closely agrees with the total hydrogen release. The slight discrepancies reflect the applied convergence tolerance of 1 in 10^5 in each grid block at each time step; with a tighter convergence tolerance and consequent use of more iterations these discrepancies could be reduced further. Subsequently there is considerably less hydrogen in the model domain than had been produced, indicating that some of the produced hydrogen escaped at the boundaries. This behavior is consistent with the simulated flow velocities. At t = 200 years, the pore velocity for upward liquid flow above the repository is approximately 0.95 m/year. The closest distance from the repository to the upper boundary is 180 m, so that the first arrival of dissolved hydrogen at the boundary is expected after about 200 years.

4.0. FRACTURED-POROUS MEDIUM

A porous medium description of the formations implies that the hydrogen released by corrosion will be (locally) uniformly distributed throughout the void space. However, if most of the permeability of the medium is provided by fractures, the hydrogen gas will tend to accumulate and migrate primarily in the fractures, and will only slowly invade the less permeable matrix blocks. It is conceivable that the response to corrosive gas release may be quite different under these conditions as compared to the porous medium idealization. A fractured-porous medium model was developed to serve as a baseline case for examining the impact of formation heterogeneities on repository behavior.

4.1. Approach

Several different approaches are available for modeling flow in fractured-porous media. Conceptually, the most straightforward approach is to explicitly include fractures into a numerical model by defining suitably small volume elements with large permeability. This approach is only applicable, however, for idealized systems with a few fractures, because the computational effort becomes unmanageable when there are many fractures present. The most popular approach for modeling systems with many fractures is the double porosity technique (Barenblatt et al., 1960; Warren and Root, 1963). In this method, a fractured-porous medium is partitioned

into (1) a primary porosity, which consists of small pores in the rock matrix, e.g., intergranular vugs or vesicles, and (2) a secondary porosity, consisting of fractures and joints. Each of the two porosities is treated as a porous continuum, whose properties can be characterized by means of the customary porous medium properties, such as permeability, porosity, and compressibility. Flow within each continuum is assumed to be porous flow, governed by Darcy's law.

In the classical double-porosity work it was assumed that global flow in the medium occurs only through the fracture continuum, while the role of the matrix rock is restricted to exchanging fluid locally with the fractures. Furthermore, the "interporosity flow" between matrix and fractures was approximated as being quasi-steady. Subsequently, "dual permeability" approaches have been developed (Miller and Allman, 1986; Dean and Lo, 1986), which permit global flow in both fracture and matrix continua. The double porosity method has also been extended to a method of "multiple interacting continua" (MINC; Pruess and Narasimhan, 1982, 1985), which can describe fully transient interporosity flow by means of suitable subgridding of the matrix blocks. The MINC-method can incorporate global flow in the matrix in the direction of fracturing while maintaining the simple one-dimensional approximation to interporosity flow (Pruess, 1985). An unrestricted description of global flow combined with a fully transient treatment of interporosity flow, however, would require at least a two-dimensional representation of flow in the matrix blocks, and would thus greatly enhance the number of grid blocks and the computational work.

In the present problem it is expected that substantial phase segregation may take place between matrix and fractures, with gas phase preferentially occupying the large voids in the fractures, and liquid phase residing preferentially in the small pores in the matrix. Therefore, it will be necessary to permit global flow in both matrix and fractures. Furthermore, because of small matrix permeability and large (of order 10 m) matrix block dimensions, it is expected that the transient periods for interporosity flow may be long. Thus the problem presents the most complicated kind of fractured-porous flow problem, where both unrestricted global flow and fully transient interporosity flow should be permitted. However, a model representing global flow in both

fracture and matrix continua, combined with a fully transient treatment of interporosity flow, would at a minimum require of the order of 30 sub-blocks in each "primary" (porous medium) grid block. For the Oberbauenstock grid with 328 primary blocks, this would add up to a total of 10,000 grid blocks or more. Thus, some fairly drastic simplifications need to be made to obtain a manageable reference case.

We have idealized the fracture system as consisting of two perpendicular sets of planar vertical fractures, with spacing of 10 m. This amounts to modeling the matrix rock as consisting of tall vertical slabs of $10 \times 10\,m^2$ square cross sectional area. An areal view of the flow system is given in Figure 13. Global flow in the fracture system is unrestricted, while global flow in the matrix may occur only in the vertical direction; in addition there is local matrix-fracture inter-porosity flow (see Figure 14). This model is implemented by partitioning each block of the primary grid (see Figure 3) into two continua, representing fracture and matrix domains, respectively. Both fracture and matrix domains are treated as porous continua, with parameters as given in Table 2. All other parameters are identical to the porous medium reference case (Table 1). Gas release is assumed to occur into the fracture continuum. The computational grid of the fractured-porous system has 618 volume elements and 1135 connections (note that elements used to define the pressure boundary conditions do not require subgridding).

The main shortcomings of this reference model are (1) the neglect of global matrix-matrix flow in the horizontal direction, and (2) the inability to describe transient interporosity flow. Either of these limitations can be remedied in future modifications. Unrestricted global flow can be realized by adding horizontal matrix-matrix flow connections, while a fully transient treatment of interporosity flow can be made by appropriate subgridding of the matrix blocks. Either of these extensions appears feasible by itself; it is only when both present limitations are to be overcome simultaneously that the computational problem grows to unmanageable proportions.

4.2. Results

Results for pressures and gas saturations in the fractures at the repository level are given in
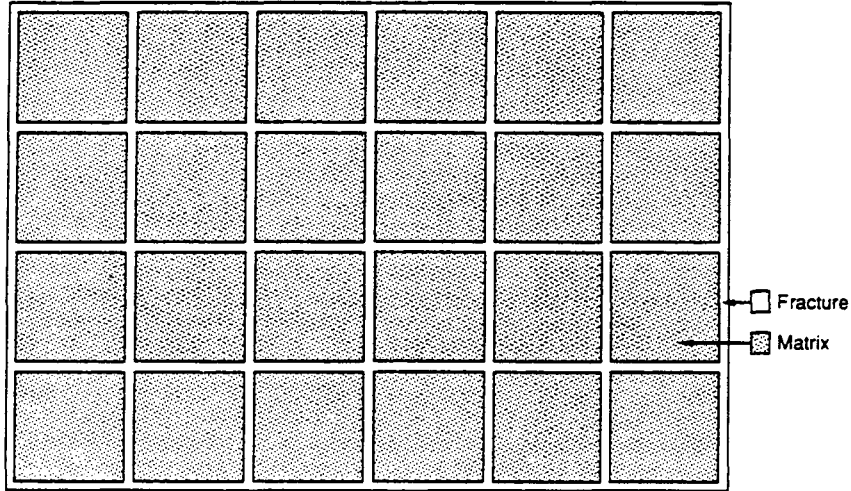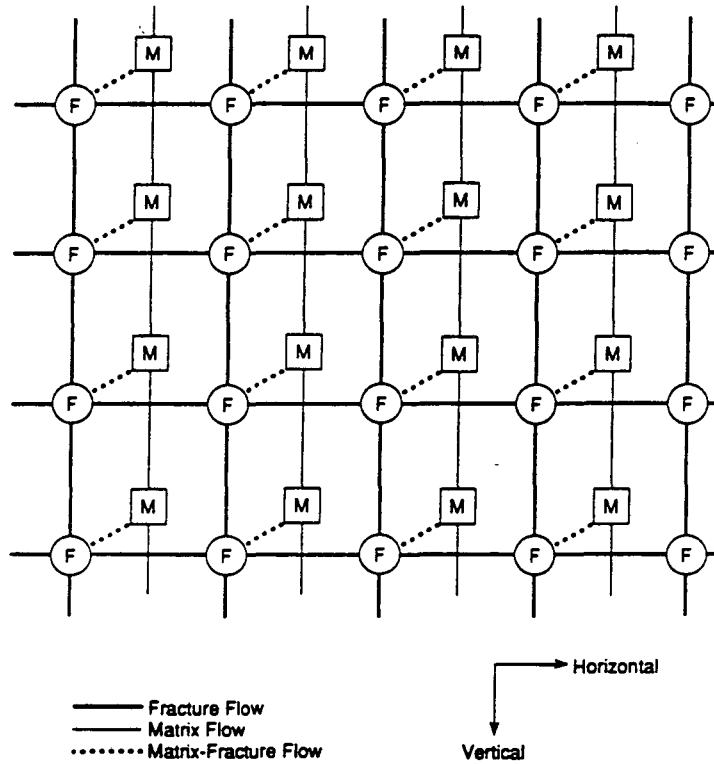
Figure 13. Schematic of fractured-porous flow system (areal view), with matrix blocks modeled as tall slabs with square cross section.

Figure 14. Schematic of flow geometry in fractured-porous model.

Figure 15. Comparison with the porous medium case shows that evolution of a free gas phase and accompanying pressurization occur at earlier time. This was expected because of the smaller average porosity of the fractures (1 %) as compared to the porous medium (3 %). Pressure increase ceases after a mobile gas saturation is reached; the maximum pressure is almost identical to that of the porous medium case. The drop in gas generation rate at t = 20 years is again accompanied by a strong pressure decline, while gas saturation continues to increase. Gas saturations in the fractured-porous medium model are generally larger than in the porous medium model, but overall the behavior of both models is remarkably similar.

The rate of gas flow from the fractures into the matrix blocks is small, and all matrix blocks remain in single phase liquid conditions for the first 100 years. After about 100 years gas begins to flow out at the top of the system, and subsequently fluid pressures decline more rapidly (see Figure 15). At the lower pressures reached after 200 years the solubility limit for hydrogen is exceeded in some matrix blocks near the repository, and a free gas phase begins to form in the matrix. Gas saturation in the matrix remains small but continues to increase as the system depressurizes, reaching maximum values of 2.5 % after 1,000 years.

The quantitative aspects of these results reflect space discretization effects. Because there is no sub-gridding in the matrix blocks, all hydrogen entering the matrix is immediately uniformly distributed throughout these blocks. A more detailed spatial resolution of flow in the matrix blocks would show that the outer "skin" of the blocks evolves some gas saturation early, while gas may take a very long time to evolve in the interior of the blocks. However, if allowance were made for capillary effects, we would expect the rock matrix with its small pores to begin to suck water out of the fractures as soon as it makes a transition to two-phase conditions. Capillary effects would thus tend to keep gas saturation in the matrix blocks to low values.

5.0. DISCUSSION AND CONCLUSIONS

The results presented in this report are to be considered illustrative and preliminary rather than quantitative, pertaining as they do to highly schematic reference cases. We have attempted to choose parameters that appear "reasonable" for the Oberbauenstock site, but it is recognized
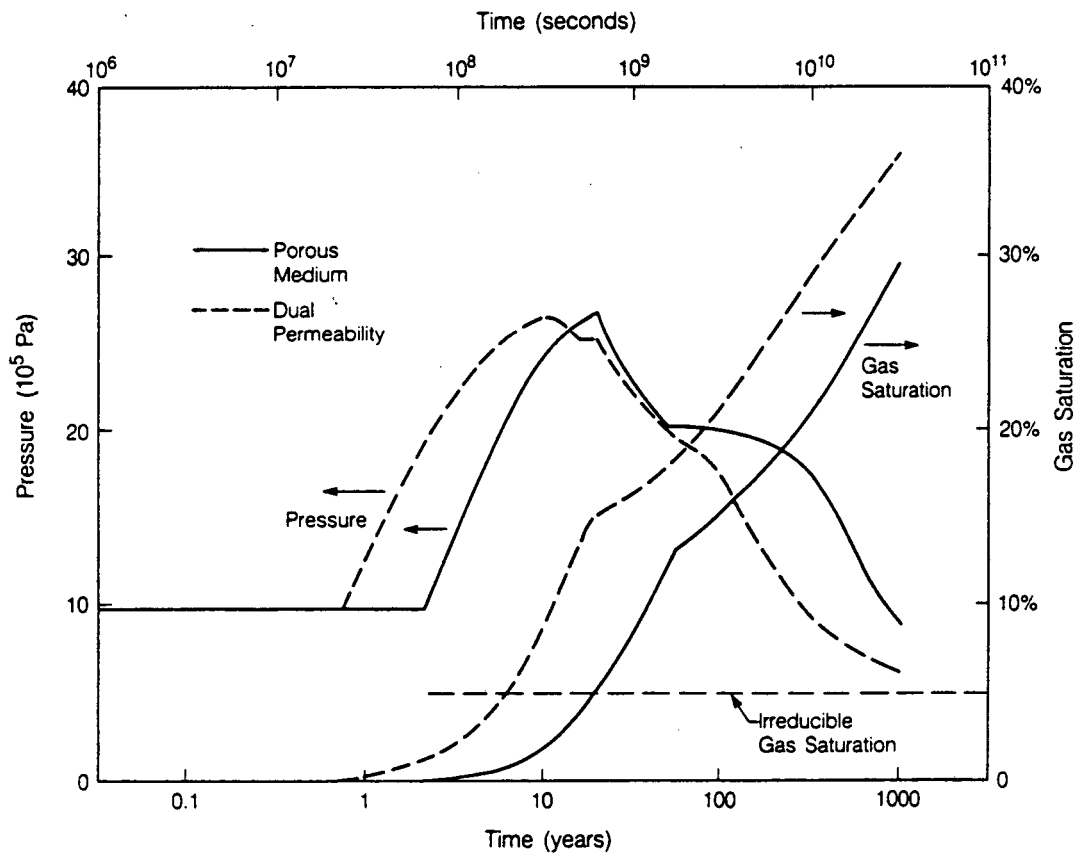
Figure 15. Predicted temporal evolution of gas pressures and saturations at the repository level. The curves labeled "dual permeability" pertain to the fractured-porous flow model.

that some of the more important parameters, such as relative permeabilities, are not well known. The porous medium reference case is not expected to provide a realistic outlook on gas pressurization and migration effects, while the fractured-porous medium case employs highly approximate descriptions of global matrix flow and interporosity flow. Another limitation of the present simulation is that rather coarse grid blocks have been used in the repository domain.

The latest results from site investigations at Oberbauenstock indicate that a few larger fracture zones exist which could have a high permeability. Additionally, it seems that some of these features are filled with natural gas. This could diminish significantly the potential pressure build-up due to gas production in the repository.

Thus, we do not wish to attach particular significance to the quantitative details of the present simulation studies. However, it appears to us that the simulation results are reasonable in a qualitative sense, showing a plausible pattern of physical processes and system behavior. Future work should focus on identifying the most important parameters affecting system behavior so that uncertainty in system response can be reduced to acceptable levels.

6.0. ACKNOWLEDGEMENT

7.0. REFERENCES

Barenblatt, G. E., Zheltov, I. P. and Kochina, I. N., Basic concepts in the Theory of Seepage of Homogeneous Liquids in Fissured Rocks, *J. Appl. Math.*, (USSR), Vol. 24, No. 5, pp. 1286-1303, 1960.

Corey, A. T., The Interrelation Between Gas and Oil Relative Permeabilities, *Producers Monthly*, pp. 38-41, November 1954.

Dean, R. H. and Lo, L. L., Development of a Natural Fracture Simulator and Examples, paper SPE-14110, presented at the SPE 1986 International Meeting on Petroleum Engineering, Beijing, China, March 1986.

Duff, I. S., MA28 - A Set of FORTRAN subroutines for Sparse Unsymmetric Linear Equations, AERE Harwell report R8730, July 1977.

Hadley, R. G., Theoretical Treatment of Evaporation Front Drying, *Int. J. Heat Mass Transfer,* Vol. 25, No. 10, pp. 1511-1522, 1982.

International Formulation Committee, A Formulation of the Thermodynamic Properties of Ordinary Water Substance, IFC Secretariat, Düsseldorf, Germany, 1967.

Klinkenberg, L. J., The Permeability of Porous Media to Liquids and Gases, in: API Drilling and Production Practice, pp. 200-213, 1941.

Knudsen, M., Die Gesetze der Molekularstroemung und der inneren Reibungsstroemung der Gase durch Roehren, *Annalen der Physik,* Vol. 28, pp. 75-131, 1909.

Miller, J. D. and Allman, D. W., Dual Permeability Modeling of Flow in a Fractured Geothermal Reservoir, Proceedings, Eleventh Workshop Geothermal Reservoir Engineering, Stanford University, Stanford, CA, pp. 77-84, January 1986.

Narasimhan, T. N., and Witherspoon, P. A., An Integrated Finite Difference Method for Analyzing Fluid Flow in Porous Media, *Water Resources Research,* Vol. 12, No. 1, pp. 57-64, 1976.

Neretnieks, I., Some Aspects of the Use of Iron Canisters in Deep Lying Repositories for Nuclear Waste, NAGRA report NTB 85-35, February 1985.

NGB 85-07, Endlager für schwach - und mittelaktive Abfälle: Das System der Sicherheitsbarrieren, January 1985.

NGB 85-08, Endlager für schwach - und mittelaktive Abfälle: Sicherheitsbericht, January 1985.

Pruess, K., A Quantitative Model of Vapor Dominated Geothermal Reservoirs as Heat Pipes in Fractured Porous Rock, Geothermal Resources Council, Transactions, Vol. 9, part II, pp. 353-361, August 1985.

Pruess, K., TOUGH User's Guide, Nuclear Regulatory Commission, Report NUREG/CR-4645, June 1987 (also Lawrence Berkeley Laboratory Report LBL-20700, Berkeley, CA, June 1987).

Pruess, K., SHAFT, MULKOM, TOUGH: A Set of Numerical Simulators for Multiphase Fluid and Heat Flow, Geotermia, Rev. Mex. Geoenergia, Vol. 4, No. 1, pp. 185-202, 1988 (also: Lawrence Berkeley Laboratory Report LBL-24430, January 1988).

Pruess, K. and Narasimhan, T. N., On Fluid Reserves and the Production of Superheated Steam from Fractured, Vapor-Dominated Geothermal Reservoirs, *J. of Geophys. Res.,* Vol. 87, No. B11, pp. 9329-9339, 1982.

Pruess, K. and Narasimhan, T. N., A Practical Method for Modeling Fluid and Heat Flow in Fractured Porous Media, *Soc. of Petr. Eng. J.,* Vol. 25, No. 1, pp. 14-26, February 1985.

Pruess, K., Wang, J. S. Y., and Tsang, Y. W., On Thermohydrological Conditions Near High-Level Nuclear Wastes Emplaced in Partially Saturated Fractured Tuff. Part 1. Simulation Studies with Explicit Consideration of Fracture Effects, Lawrence Berkeley Laboratory Report LBL-24563, January 1988 (submitted to Water Resources Research).

Rasmuson, A. and Elert, M., The Influence of Gas Flow on Solute Transport, Kemakta AB, Stockholm, Draft Report to NAGRA, October 1986.

Resele, G. and Tripet, J. P., Hydrogeologische Grundlagen für das Modellgebiet Oberbauenstock, NAGRA report NTB 85-29, April 1985.

Vargaftik, N. B., Tables on the Thermophysical Properties of Liquids and Gases, Second Edition, John Wiley and Sons, New York, 1975.

Walker, W. R., Sabey, J. D. and Hampton, D. R., Studies of Heat Transfer and Water Migration in Soils, Final Report, Department of Agricultural and Chemical Engineering, Colorado State University, Fort Collins, CO, April 1981.

Warren, J. E. and Root, P. J., The Behavior of Naturally Fractured Reservoirs, *Soc. Petr. Eng. J.,* pp. 245-255, September 1963, Transactions, AIME, 228.

Wiborgh, M., Höglund, L. O., and Pers, K., Gas Formation in a L/ILW Repository and Gas Transport in the Host Rock, NAGRA Report NTB 85-17, December 1986.

APPENDIX A: Summary Description of TOUGH Simulator

TOUGH is a multi-dimensional numerical simulator for the coupled transport of water, vapor, air and heat in porous and fractured media (Pruess, 1987). It is a member of the MUL-KOM family of multi-phase, multi-component codes, which is being developed at Lawrence Berkeley Laboratory primarily for geothermal reservoir applications (Pruess, 1988). The acronym "TOUGH" stands for " transport of unsaturated groundwater and heat."

The TOUGH simulator takes account of the following physical processes. Fluid flow in both liquid and gaseous phases occurs under pressure, viscous, and gravity forces according to Darcy's law, with interference between the phases represented by means of relative permeability functions. In addition we consider binary diffusion in the gas phase. However, no account is presently made of Knudsen diffusion, which will effectively enhance gas phase permeability under conditions when the mean free path of gas molecules becomes comparable to or larger than typical pore sizes (Knudsen, 1909; Klinkenberg, 1941; Hadley, 1982). This effect will become important for media with very small pores and/or at small gas pressures. Capillary and phase adsorption effects are taken into account for the liquid phase, but no allowance is made for vapor pressure lowering, which will become significant for very strong suction pressures (for example, a suction pressure of -14.5 MPa will cause approximately 10% reduction in vapor pressure). Also, no allowance is made for hysteresis in either capillary pressure or relative permeability. All thermophysical properties of liquid water and vapor are obtained within experimental accuracy from steam table equations (International Formulation Committee, 1967). Air is treated as an ideal gas, and additivity of partial pressures is assumed for air/vapor mixtures. Air dissolution in water is represented by Henry's law. No allowance is made for diffusion of dissolved gas in

the liquid phase. This will usually be negligible because both air solubility and diffusivity in the liquid phase are small.

Heat transport occurs by means of conduction, with thermal conductivity dependent on water saturation, and convection and binary diffusion, which includes both sensible and latent heat.

The governing mass- and energy-balance equations solved by TOUGH can be written in the following general form

$$\frac{d}{dt} \int_{V_n} M^{(\kappa)} \, dV = \int_{\Gamma_n} \underset{\sim}{F}^{(\kappa)} \cdot \underset{\sim}{n} \, d\Gamma + \int_{V_n} q^{(\kappa)} \, dV \tag{1}$$

$$(\kappa = 1: \text{water}; \, \kappa = 2: \text{air}; \, \kappa = 3: \text{heat})$$

The mass accumulation terms ($\kappa = 1,2$) are

$$M^{(\kappa)} = \phi \sum_{\beta = l,g} S_\beta \, \rho_\beta \, X_\beta^{(\kappa)} \tag{2}$$

where ϕ is porosity, S_β is saturation or volume fraction of phase β (= liquid, gas), ρ_β is density of phase β, and $X_\beta^{(\kappa)}$ is the mass fraction of component κ present in phase β. Thus, $M^{(\kappa)}$ is the total mass of component κ present per unit volume of the flow system. The heat accumulation term contains rock and fluid contributions

$$M^{(3)} = (1 - \phi) \, \rho_R \, C_R \, T + \phi \sum_{\beta = l,g} S_\beta \, \rho_\beta \, u_\beta \tag{3}$$

where ρ_R is rock grain density, C_R is rock specific heat, T is temperature, and u_β is specific internal energy of phase β.

The mass flux terms contain a sum over phases

$$\underset{\sim}{F}^{(\kappa)} = \sum_{\beta = l,g} \underset{\sim}{F}_\beta^{(\kappa)} \tag{4}$$

where the flux in each phase is

$$\underset{\sim}{F}_\beta^{(\kappa)} = -k \, \frac{k_{r\beta}}{\mu_\beta} \, \rho_\beta \, X_\beta^{(\kappa)} \, (\nabla P_\beta - \rho_\beta \, \underset{\sim}{g}) - \delta_{\beta g} \, D_{va} \, \rho_\beta \nabla \, X_\beta^{(\kappa)} \tag{5}$$

Here k is absolute permeability, $k_{r\beta}$ is relative permeability of phase β, μ_β is viscosity of phase β, $P_\beta = P + P_{cap,\beta}$ is the pressure in phase β (sum of a reference phase pressure and capillary pressure), and g is gravitational acceleration. $\delta_{\beta g}$ is the "Kronecker delta," being equal to 1 for phase β = gas and 0 otherwise. Thus no allowance is made for diffusion of dissolved gas in the liquid phase. D_{va} is the diffusion coefficient for vapor-air mixtures (Vargaftik, 1975; Walker et al., 1981),

$$D_{va} = \tau \, \phi \, S_g \, D_{va}^o \, \frac{P_o}{P} \left[\frac{T + 273.15}{273.15} \right]^\theta \tag{6}$$

where τ is a tortuosity factor, which is dependent on pore geometry. D_{va}^o is the air-vapor diffusion coefficient at standard conditions of $P_o = 1$ bar, $T_o = 0°C$, and $\theta \approx 1.80$ is a material parameter.

Heat flux contains conductive and convective components

$$\underset{\sim}{F}^{(3)} = - K \nabla T + \sum_{\substack{\beta = l, g \\ \kappa = 1,2}} h_\beta^{(\kappa)} \, \underset{\sim}{F}_\beta^{(\kappa)} \tag{7}$$

Here K is heat conductivity of the rock-fluid mixture, and h_β is specific enthalpy of phase β.

The transport equations given above need to be complemented with constitutive relationships, which express all parameters as functions of a set of primary thermodynamic variables. The thermophysical properties of water substance are accurately represented by the steam table equations, as given by the International Formulation Committee (1967). Air is represented as an ideal gas. For the present problem TOUGH was modified so that the non-condensible gas represents hydrogen rather than air. The modifications affect density, viscosity, and water solubility of the gas (see Table 4).

For numerical solution the integro-differential Equations (1) are discretized, using first-order finite differences in time and integral finite differences for the space variables (Narasimhan and Witherspoon, 1976). For numerical stability all flux terms are evaluated "fully implicitly," i.e., at the advanced time level. It is assumed that the flow system is in thermodynamic

equilibrium locally, so that conditions in each volume element of the finite difference grid can be uniquely characterized by a complete set of thermodynamic state variables. The thermodynamic state variables are pressure, temperature, and mass fraction of non-condensible gas in single-phase conditions, and pressure, temperature, and gas saturation in two-phase conditions.

Discretization results in a set of non-linear coupled algebraic equations. These are solved by means of Newton-Raphson iteration. The linear equations arising at each iteration step are solved with a sparse version of Gaussian elimination (Duff, 1977).

LAWRENCE BERKELEY LABORATORY
UNIVERSITY OF CALIFORNIA
INFORMATION RESOURCES DEPARTMENT
BERKELEY, CALIFORNIA 94720